AFRL-RZ-WP-TP-2008-2038

TRANSIENT PLASMA INDUCED PRODUCTION OF OH AND ITS EFFECTS ON IGNITION IN ATMOSPHERIC CH$_4$-AIR QUIESCENT MIXTURES (POSTPRINT)

Charles Cathey, Jeremy Cain, Hai Wang, Martin A. Gundersen, Michael Ryan, and Campbell D. Carter

Propulsion Sciences Branch
Aerospace Propulsion Division

JANUARY 2008

STINFO COPY

AIR FORCE RESEARCH LABORATORY
PROPULSION DIRECTORATE
WRIGHT-PATTERSON AIR FORCE BASE, OH 45433-7251
AIR FORCE MATERIEL COMMAND
UNITED STATES AIR FORCE

REPORT DOCUMENTATION PAGE

Form Approved
OMB No. 0704-0188

1. REPORT DATE *(DD-MM-YY)*	2. REPORT TYPE	3. DATES COVERED *(From - To)*
January 2008	Conference Paper Postprint	30 April 2004 – 01 November 2007

4. TITLE AND SUBTITLE

TRANSIENT PLASMA INDUCED PRODUCTION OF OH AND ITS EFFECTS ON IGNITION IN ATMOSPHERIC CH_4-AIR QUIESCENT MIXTURES (POSTPRINT)

5a. CONTRACT NUMBER
In-house

5b. GRANT NUMBER

5c. PROGRAM ELEMENT NUMBER
61102F

6. AUTHOR(S)

Charles Cathey, Jeremy Cain, Hai Wang, and Martin A. Gundersen (University of California)
Michael Ryan (Universal Technology Corporation)
Campbell D. Carter (AFRL/RZAS)

5d. PROJECT NUMBER
2308

5e. TASK NUMBER
AI

5f. WORK UNIT NUMBER
2308AI00

7. PERFORMING ORGANIZATION NAME(S) AND ADDRESS(ES)

University of Southern California
Los Angeles, CA 90089

Universal Technology Corporation
Dayton, OH 45432

Propulsion Sciences Branch (AFRL/RZAS)
Aerospace Propulsion Division
Air Force Research Laboratory, Propulsion Directorate
Wright-Patterson Air Force Base, OH 45433-7251
Air Force Materiel Command, United States Air Force

8. PERFORMING ORGANIZATION REPORT NUMBER
AFRL-RZ-WP-TP-2008-2038

9. SPONSORING/MONITORING AGENCY NAME(S) AND ADDRESS(ES)

Air Force Research Laboratory
Propulsion Directorate
Wright-Patterson Air Force Base, OH 45433-7251
Air Force Materiel Command
United States Air Force

10. SPONSORING/MONITORING AGENCY ACRONYM(S)
AFRL/RZAS

11. SPONSORING/MONITORING AGENCY REPORT NUMBER(S)
AFRL-RZ-WP-TP-2008-2038

12. DISTRIBUTION/AVAILABILITY STATEMENT
Approved for public release; distribution unlimited.

13. SUPPLEMENTARY NOTES
Conference paper published in the Proceedings of the 46th AIAA Aerospace Sciences Meeting and Exhibit.
Report contains color. PAO Case Number: WPAFB 07-0549, 29 Nov 2007.

14. ABSTRACT

Transient plasma from a 60 kV, 70 ns pulse induced OH production in air and CH_4/air quiescent mixtures inside a cylindrical chamber is analyzed. The resulting OH from the plasma discharge, ignition, and subsequent combustion is analyzed using planar laser induced fluorescence. A high-framing-rate camera was also used to image ignition and flame propagation in the chamber, providing spatial and temporal resolution over the entire combustion event. Results indicate OH structures produced during the discharge in humid, ambient air are less branched, thicker, and last longer when compared to structures in CH_4/dry-air. Transient plasma successfully ignited the CH_4/air mixture, populating the discharge volume with radicals. Mean OH number densities produced by the discharge were found to decay within 100 µs of the plasma. Ignition under these conditions was found to occur approximately 1 ms after the discharge along the anode, creating multiple ignition kernels whose proximity to the anode is consistent with the region of highest field and, thus, maximum radical density.

15. SUBJECT TERMS

16. SECURITY CLASSIFICATION OF:

a. REPORT	b. ABSTRACT	c. THIS PAGE
Unclassified	Unclassified	Unclassified

17. LIMITATION OF ABSTRACT:
SAR

18. NUMBER OF PAGES
16

19a. NAME OF RESPONSIBLE PERSON (Monitor)
Campbell D. Carter

19b. TELEPHONE NUMBER *(Include Area Code)*
N/A

Standard Form 298 (Rev. 8-98)
Prescribed by ANSI Std. Z39-18

Transient Plasma Induced Production of OH and its Effects on Ignition in Atmospheric CH₄–Air Quiescent Mixtures

Charles Cathey,[1] Jeremy Cain,[2] Hai Wang,[3] and Martin A. Gundersen[4]
University of Southern California, Los Angeles, Ca 90089

Michael Ryan[5]
Universal Technology Corporation, Dayton, OH 45432

Campbell D. Carter[6]
Air Force Research Laboratory, Propulsion Directorate, Wright-Patterson AFB, OH 45433

This paper analyzes transient plasma induced OH production in air and CH₄/air quiescent mixtures inside a cylindrical chamber. The chamber is filled with ambient air or a CH₄/dry-air mixture, and a 60 kV electrical pulse 70 ns in duration is sent through a steel rod at the axis of the chamber. A highly transient corona discharge forms between the central electrode and the chamber walls. The resulting OH from the plasma discharge, ignition, and subsequent combustion is analyzed using planar laser induced fluorescence. A high-framing-rate camera was also used to image ignition and flame propagation in the chamber, providing spatial and temporal resolution over the entire combustion event. Results indicate OH structures produced during the discharge in humid, ambient air are less branched, thicker, and last longer when compared to structures in CH₄/dry-air. Transient plasma successfully ignited the CH₄/air mixture, populating the discharge volume with radicals. Mean OH number densities produced by the discharge were found to reach $\sim 4 \times 10^{14}$ cm^{-3} and decay within 100 μs of the plasma. Ignition under these conditions was found to occur approximately 1 ms after the discharge along the anode, creating a cylindrically expanding flame front. Transient plasma ignition was found to be a truly volumetric ignition source, creating multiple ignition kernels whose proximity to the anode is consistent with the region of highest field and, thus, maximum radical density. Additionally, the rapid decay of the initial OH (as seen by the pump beam) with respect to the time of ignition suggests that the anode itself may have an important role in affecting combustion kinetics.

I. Introduction

T he formative, non-equilibrated phase of a plasma prior to arc formation, referred to as transient plasma hereafter, has strong potential as an ignition source on a variety of platforms. What makes transient plasma ignition (TPI) attractive as an ignition source for most engines is its ability to reduce ignition delay over broad ranges of temperature and pressure and to enable combustion of leaner mixtures.[1] While there has been substantial experimental work done on using transient plasmas for ignition, very little research addresses the underlying combustion-plasma physics.[2,3] This presentation shows streamer-induced radical (OH) production during transient plasma discharge, as well as high speed imaging of the resulting flame front.

---

[1] PhD. Student, Department of Electrical Engineering - Electrophysics, AIAA Student Member.

[2] PhD. Student, Department of Aerospace and Mechanical Engineering.

[3] Professor, Department of Aerospace and Mechanical Engineering.

[4] Professor, Department of Electrical Engineering - Electrophysics, AIAA Member.

[5] Research Scientist, Universal Technology Corporation, AIAA Member.

[6] Senior Aerospace Engineer, Propulsion Directorate, AIAA Associate Fellow.

Although the effect of initial radical production by the streamers in transient plasma is not well characterized, it is expected that the higher fraction of energetic electrons during the transient phase will enhance ionization and the number of electron-impact dissociation reactions. Key to combustion of hydrocarbons (RHs) are the formation of atomic/free radical species O, OH, and H.[4] Chain initiation occurs in gaseous hydrocarbons via hydrogen abstraction by molecular oxygen:

$$RH + O_2 \rightarrow R + HO_2 \tag{1}$$

It is important to note that the reaction rate constants usually have an exponential dependence on temperature via Arrhenius' law. It is thought that transient plasmas generate the initial radical pool via electron-impact dissociation and ionization. The initiation reaction (1) is replaced with the electron-impact dissociation reactions of (2) and (3):

$$RH + e \rightarrow R + H + e \tag{2}$$

$$O_2 + e \rightarrow O + O + e \tag{3}$$

Reactions (2) and (3) are examples of what is believed to occur when a non-equilibrated plasma in the form of a fast ionization wave or a transient plasma is applied to the mixture.[5,6] There is a large difference in reaction rate values between the more conventional thermal chain initiation equation (1) and those of (2) and (3), with the electron-impact reactions being much faster. Another consideration is that in the case of electron-impact dissociation the reaction rate constant is independent of temperature but dependent on the *reduced electric field,* defined as the electric field divided by the total gas number density (E/N). This process of electron-impact dissociation is thought to occur over the streamer paths, with the highest density of hydrocarbon fragments generated at the point of highest field near the anode.

II. Experimental Setup

This experiment consists of a Planar Laser Induced Fluorescence (PLIF) measurement to probe OH development and production induced by the transient plasma and a high-speed imaging component to track flame propagation. The inset in Fig. 1 depicts the cylindrical combustion chamber used in the experiment. The main imaging window is 10.16 cm diameter, 2.54 cm thick fused silica; while the laser entry and exit windows are 2.54 cm in diameter (sapphire), the corresponding holes in the chamber are simple slits (2.5 cm high) machined into the cylindrical wall. This provides minimal intrusion as far as stream propagation is concerned. The chamber is 10.16 cm inner diameter, 20.32 cm long stainless steel. The anode is an 8-32 threaded rod, 7.62 cm long. It is important to note that during the combustion process water vapor is a product and condensation on the windows can be a problem. Because condensation only becomes a problem in post-ignition work and this experiment is primarily focused on the radical production prior to ignition, no heaters were used to prevent condensation on the windows during the imaging process. The initial conditions for the chamber (for combustion experiments) were 1) a mixture of stoichiometric CH_4 (chemically pure grade) and dry air, 2) a pressure of 101 kPa, and 3) a nominal temperature of 293 K. The mixture was prepared by first evacuating the chamber, then introducing the specified partial pressure of CH_4, then introducing the specified partial pressure of air, and finally waiting to allow the gases to thoroughly mix. A set of measurements with "humid" air are also described below. In this case room air was allowed to fill the chamber (after evacuation); the room air had a relative humidity of ~2%, and the ambient pressure was 99 kPa.

A line-type *pseudospark* switched pulse generator charged with a Glassman High Voltage DC supply was used to create a 70 ns FWHM, 60 kV pulse, resulting in the transient plasma.[6] Chamber pressure was monitored with an Omega PX-105 piezoelectric pressure transducer. Spark ignition, for reference purposes, was accomplished using a conventional car sparkplug (Champion RV17YC6) and a commercially available automobile ignition circuit, which created a discharge of ~40 mJ. For spark ignition tests the transient plasma electrode was removed and replaced with the sparkplug, which was put in the center of the plate opposite the main viewing window.
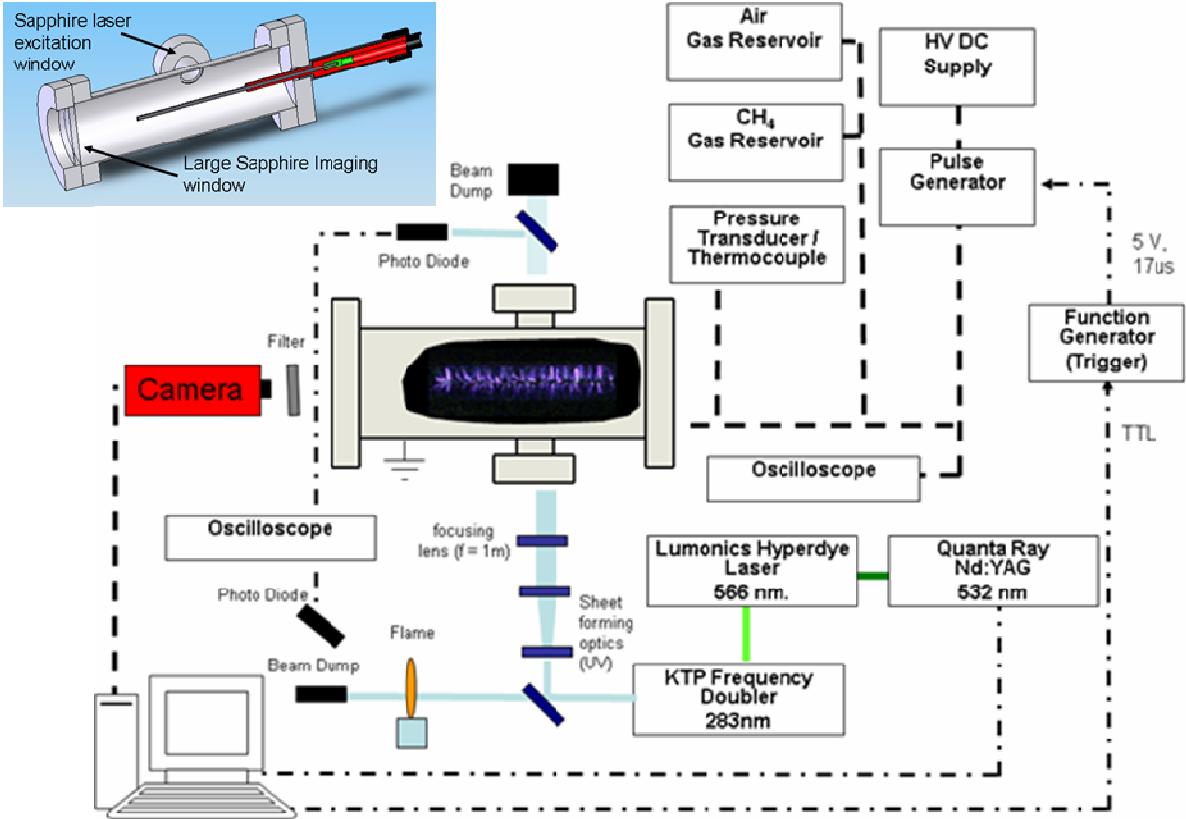
Figure 1. Schematic of the OH-PLIF experiment.

The experimental setup is shown in Fig. 1. An injection-seeded, pulsed Nd:YAG (Spectra-Physics GCR-170) laser was used to pump a dye laser, which was then frequency doubled to generate the beam at 282 nm. Specifically, the output of the frequency doubled Nd:YAG laser (400 mJ-per-6 ns pulse) pumps a Lumonics Hyperdye HD-300 dye laser to produce ~80 mJ/pulse at 564 nm. The 564 nm beam was then passed through a frequency doubler (Inrad Autotracker III) to obtain 282 nm radiation. The 282 nm beam was then separated from the dye beam with an Inrad Prism Harmonic Separator. The laser probe sheet was formed using a combination of cylindrical (-100 mm focal length) and spherical lenses (1 m focal length). The sheet height was apertured by the 2.5 cm high window slit, and the sheet thickness is estimated to be 300 μm. The reflection from the front surface of the plano-concave cylindrical lens was directed over a small *reference* flame (a 2.5 cm diameter McKenna burner) and then to a photodiode. A photomultiplier tube monitored the dye laser tuning by a fluorescence signal from the flame and the photodiode monitored the laser energy, both via a digital oscilloscope. Additionally, a second beam pick-off at the exit window of the chamber was set up to monitor extinction of the beam due to condensation on the windows during combustion.

The OH fluorescence from the chamber was collected by a PIMAX UV sensitive (Superblue) intensified CCD camera with a Cerco 45 mm focal length f/1.8 UV lens. The camera gate was normally set to 200 ns, but was also set as low as 50 ns to reduce collection of the discharge emission. Furthermore, the camera's *bracket pulsing* option was used to further reduce the collected emission from the discharge.

For the fluorescence imaging the OH was excited by pumping a transition in the $A^2\Sigma^+ \leftarrow X^2\Pi$ (v′=1,v″=0) band. UG-5 and WG-305 Schott-glass filters were used to isolate the (v′=1,v″=1)- and (0,0)-band fluorescence signal from the (1,0) fluorescence and 282 nm scattering. The transient plasma deposits a small amount of energy (~800 mJ) to the mixture; also, the short plasma duration (pulse width ~70 ns) does not allow the plasma to reach thermal equilibrium ($T_e \approx T_{gas}$). When taken together one can assume that there is negligible heating of the gas by the transient plasma. Therefore, assuming a gas temperature of 300 K within the streamers, the $Q_1(3)$ transition at 282.209 nm was chosen for excitation, as its ground state offers a reasonable compromise between low-temperature population and insensitivity to temperature changes at low temperatures.

OH number densities in the streamers were estimated by imaging OH fluorescence in a 2.54 cm square Hencken burner as a calibration, similar to the method used by Barlow et al.[8] Previously, Ombrello et al.[9] showed through

absorption measurements that the OH number density in the burnt gas region of a premixed CH_4–air flame is $(0.94 \pm 0.07) \times 10^{16}$ cm^{-3}, a value consistent with a burnt gas temperature of 2170 K. The ratio of fluorescence signals in the chamber and Hencken flame, along with the number density in the Hencken flame, allowed estimation of the discharge number densities.

The formula used to calculate the number density is:

$$N_{OH,reactants} = N_{OH,Hencken} \cdot \left(\frac{S_{f,reactants}}{S_{f,Hencken}} \right) \cdot \left(\frac{\hat{F}_{Hencken}}{\hat{F}_{reactants}} \right) \cdot \left(\frac{f_{B,Hencken}}{f_{B,reactants}} \right) \qquad (4)$$

Here, *reactants* indicates conditions during the transient plasma, *Hencken* indicates conditions in the Hencken flame, N_{OH} is the total number density of OH, S_f is the fluorescence signal detected by the camera, and f_B is the Boltzmann fraction. $\hat{F}$ is the *specific fluorescence,* defined as

$$\hat{F} \equiv \frac{\int_{\Delta t} \left(N_1 \varepsilon_1 A_1 + N_0 \varepsilon_0 A_0 \right) \cdot dt}{f_B N_{OH}} \,, \qquad (5a)$$

which for linear fluorescence conditions becomes

$$\hat{F} = \int_{\Delta t} W dt \cdot \left(\frac{\varepsilon_1 A_1 + \varepsilon_0 A_0 Q_{V,10} / \left(Q_{e,0} + A_0 \right)}{Q_{V,10} + Q_{e,1} + A_1} \right) \qquad (5b)$$

Here, N_i, ε_i, A_i and $Q_{e,i}$ are the number density, fluorescence collection efficiency, fluorescence rate, and electronic quenching rate for the A-state $v' = i$ (0 or 1) level, respectively. $Q_{V,10}$ is the rate for VET from $v' = 0$ to 1 and W is the laser excitation rate, whose integral in time is proportional to the laser pulse energy. Note that in deriving Eq. (5b) it is assumed that upward VET, from $v' = 0$ to 1 or from $v' = 1$ to 2, is negligibly small. The fluorescence rates A_0 and A_1 are taken from Luque and Crosley,[10] collision rates $Q_{e,1}$, $Q_{e,0}$, and $Q_{V,10}$ are from Steffens and Crosley[11] for the CH_4/air mixture (low-temperature), and from Köllner et al.[12] and Paul,[13] for the Hencken-burner calibration flame. It is important to emphasize that the two conditions, the burnt gas and the combustible mixture, are very different collisional environments, and a more suitable low temperature calibration condition is desired.

It is assumed that the fluorescence is in the linear regime. However, based on estimated laser sheet irradiance of ~6.7×10^{10} W/m^2 and the derived excitation rate ~5×10^9 s^{-1}, some degree of transition saturation exists, particularly for the flame conditions. To better understand the role of transition saturation, the excitation and energy exchange processes were modeled with a set of rate equations. This was accomplished with a 5-level model representing the populations of the directly pumped rovibronic levels, $X(v'' = 0, N=3)$ and $A(v' = 1, N = 3)$, the remaining rotational states of the $A(v' = 1)$ and $X(v'' = 0)$ levels, and the $A(v' = 0)$ level. A representative diagram can be seen in Fig. 2. Of course, rotational energy transfer rates are also needed calculate the population exchange with the directly pumped ro-vibronic levels and surrounding levels; these rates were thus determined from Kliner and Farrow,[14] Burris et al.,[15] and Zizak et al.[16] As the excitation rate increases from low values to ~5×10^9 s^{-1}, the ratio $\hat{F}_{Hencken} / \hat{F}_{reactants}$ increases only modestly from a value of 2.4 based on Eq. (5b). A value of $\hat{F}_{Hencken} / \hat{F}_{reactants} \approx$ 2.4 (± 0.8) is assumed to be a reasonable approximation, where the uncertainty is based on the uncertainty in collision rates coupled with that produced by transition saturation effects.
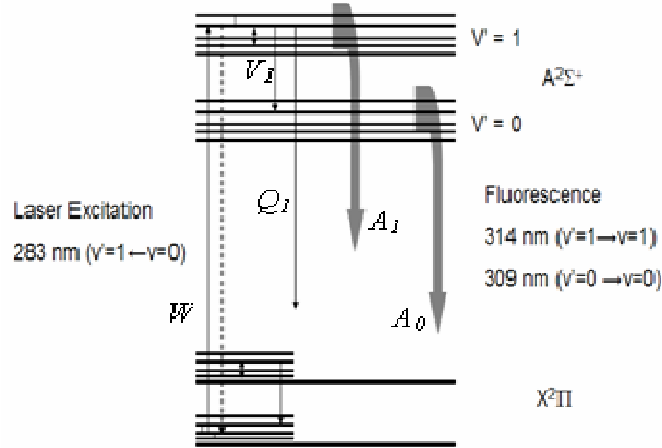
Figure 2. Diagram of electronic states and energy levels of OH employed in OH number density measurements. *W* **indicates the absorption process,** Q_e **the electronic quenching process,** $Q_{V,10}$ **the vibrational energy transfer process, and** *A* **the fluorescence process.**

For the high-speed imaging of the flame front, the experimental setup was essentially that in Fig. 1 without a laser. The Princeton Instruments camera was replaced with a Photron FASTCAM-Ultima APXi2 intensified high speed camera. Images were recorded with both CH- (centered at 430 nm with a pass band of 10 nm, FWHM) and OH-emission line filters (centered at 307 nm with a pass band of 25 nm, FWHM) at 2000 frames-per-second. In addition, the field of view of the camera was adjusted from the PLIF experiment such that the camera was able to image the entire discharge volume.

III. Results and Discussion

A. OH PLIF

Figure 3 shows a pseudo time series of OH PLIF images during and after the transient plasma in stoichiometric CH_4/air mixtures. The field of view is the top left quadrant of the cylinder, which was a compromise between view extent and resolution. The laser travels from right to left. In some of the images background scatter from the anode mount is seen as a circle around the anode. It is more easily seen when the OH signal is low, and is the residual from background subtraction. Each image in the series is taken from a separate firing of the chamber. The transient plasma induces OH production along the streamer discharge path. There is a short delay between when the discharge ends and OH begins to appear. Very little OH fluorescence is seen at 90 ns. At 160 ns the OH signal is at its greatest and decays steadily afterwards. The OH produced is seen to fall below the detection limit of the apparatus beyond 100 µs. Ignition occurs approximately 1 ms after the plasma initiation along the length of the anode, creating an expanding cylindrical flame. The OH population does not appear to have a direct effect on ignition, as ignition occurs long after peak number densities are reached and the OH density is no longer detectable.
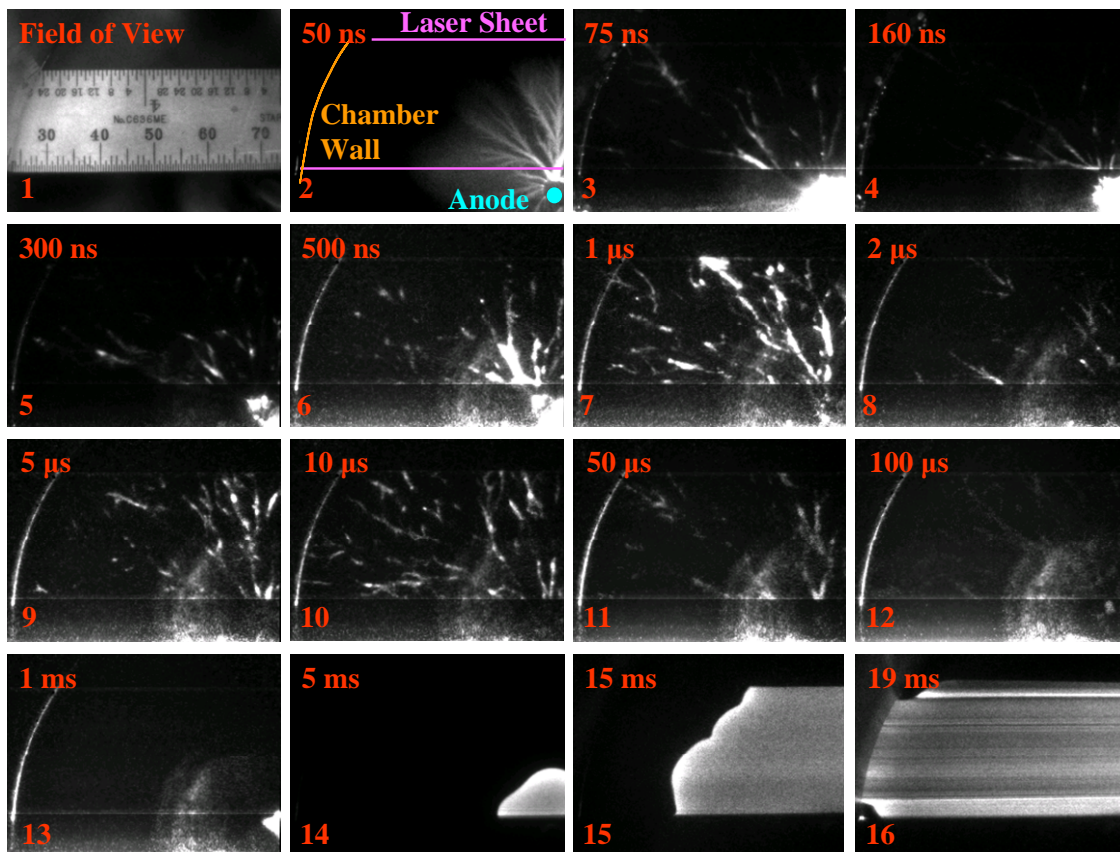
Figure 3. OH-PLIF images during CH$_4$/air combustion, ϕ = 1. Intensity scaling was adjusted for maximum viewability.

Figure 4 is a decay curve of the OH number densities induced by the plasma. These were calculated by thresholding the image to distinguish between the fluorescence signal and background. The mean value was determined by summing the number densities at each pixel with signal above the threshold value and dividing it by the number of pixels with signal. The peak mean number densities are greatest shortly after the plasma discharge, where they reach ~4×10^{14} cm^{-3}. Afterwards the peak mean number density decays until it reaches the detection limit at approximately 100 µs. This is long before the normal ignition time of 1 ms. It is important to note that while the mean values are on the order of 10^{14} cm^{-3}, there are spots within the OH structures where OH levels are higher by an order of magnitude or more (see inset in Figure 4).
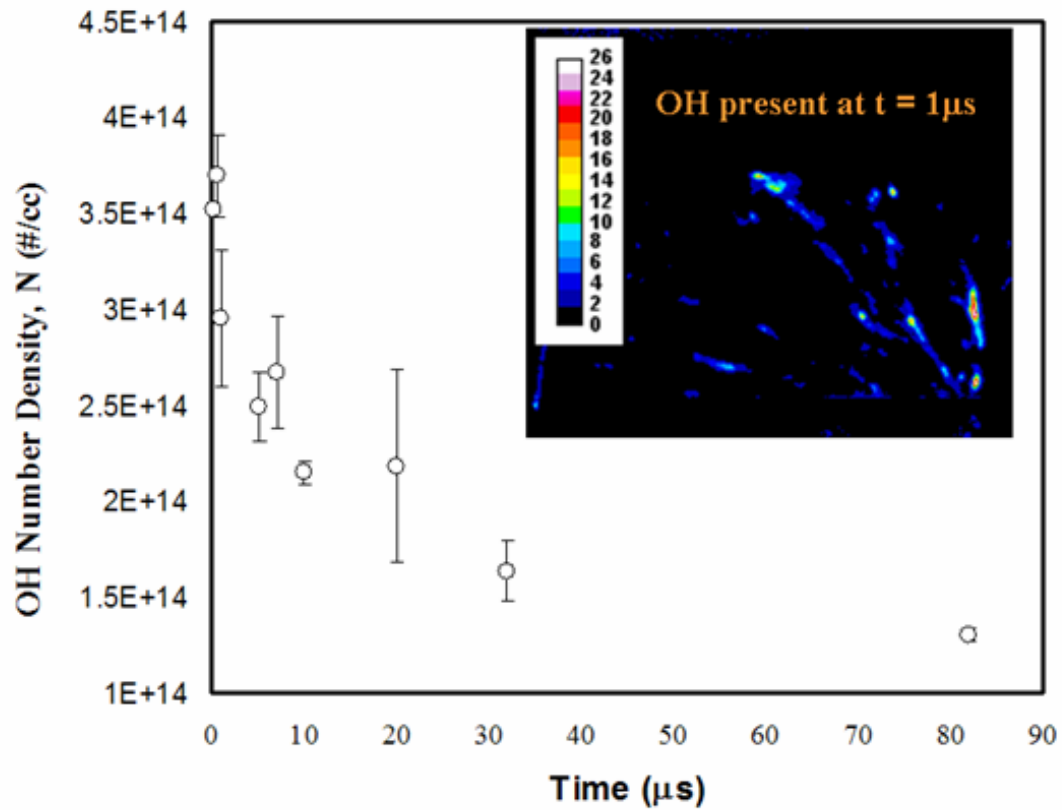
American Institute of Aeronautics and Astronautics

Figure 4. OH decay curve. The inset is a PLIF image calibrated to show OH number density at t=1 μs, with values of order 10^{14} molecules/cm^{-3}.

Figure 5 shows OH production using room air (instead of dry air) with a pseudo-time history of PLIF images. It was found that OH produced in room air (~2% relative humidity) persisted much longer (~500 μs) and decayed differently than that in the CH_4/dry-air mixture. The OH produced in humid air follows a less branched pattern and is initially of diameter 2-5 mm, versus ~1 mm in the case of CH_4/air. Afterwards, the region of high OH concentration appears to expand outward from the original thin streamers.
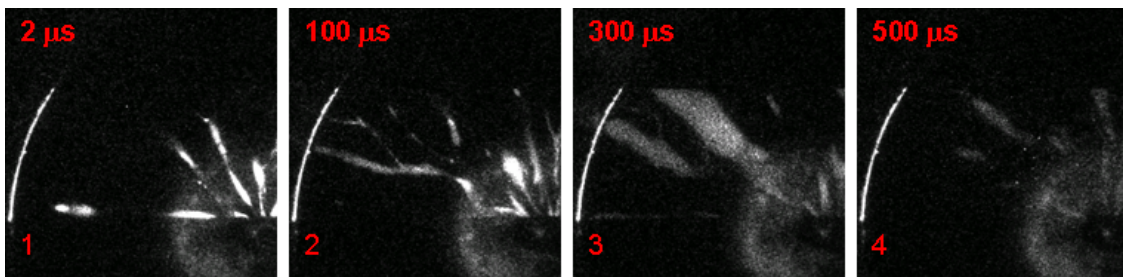

Figure 5. OH-PLIF images in humid ambient air. Intensity scaling was held constant for the four images.

B. High Speed Imaging

Figure 6 shows high-speed images taken through the CH-emission filter during and after ignition in stoichiometric CH_4/air mixtures. Time series were taken using both conventional spark and transient plasma ignition. The difference in flame geometries is important to note between the transient plasma and the spark ignited systems. The conventional spark plug can be assumed to be a point source when compared to the transient plasma. Additionally the spark plug kernel creates an expanding hemispherical flame that grows along the rear wall of the chamber and then propagates forward towards the camera. The transient plasma ignited flame begins at multiple ignition points surrounding the ~75 mm long 8-32 threaded rod, all at about 1 ms. These multiple flame fronts

American Institute of Aeronautics and Astronautics

propagate outward towards the chamber wall. When the transient plasma ignited flame reaches the chamber wall (t ≈ 20 ms) it has combusted ~ 40% of the chamber volume, whereas at the same time the spark ignited flame has not left the rear chamber wall. The wall contact is important because it acts as sink for heat and radicals and retards increases in flame temperature and speed. In examining the transient plasma ignited flame, there appears to be some wrinkling of the flame front. This is likely due to multiple ignition kernels along the anode surface and possibly due to slightly different fluid composition where the plasma streamers were located. It is also possible that wrinkling at large radii is caused by concentration gradients across the surface, which increase the rate of diffusive mixing across the flame front.[17]
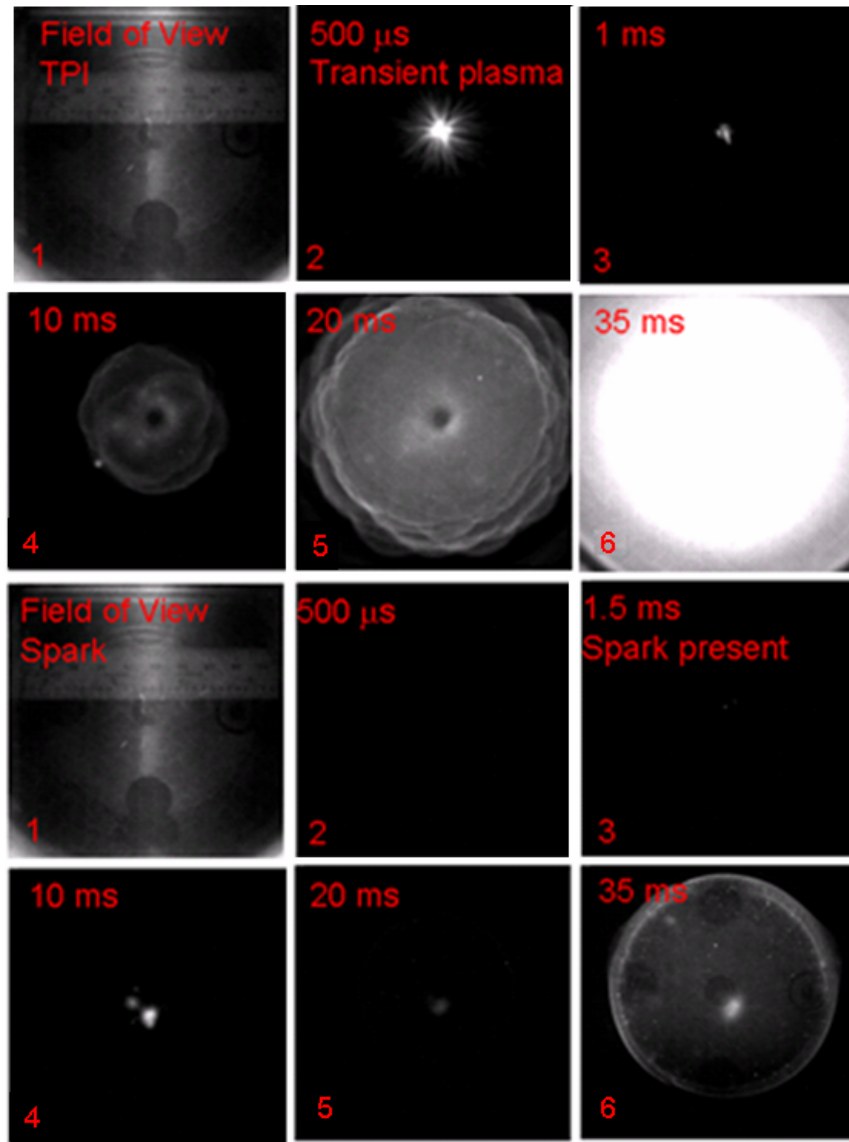

Figure 6. High-speed camera images using the CH-emission filter. The first two rows depict flame propagation when transient plasma is the ignition source. The bottom two rows show flame propagation ignited by a traditional spark plug located on the back wall. The camera was gated such that exposure for each frame is 500 μs.

There are several possible explanations as to why ignition is solely occurring along the anode during TPI. The first and perhaps simplest is that this is the region of highest field and, therefore, highest radical production. Recall that the coaxial geometry produces a highly non-uniform electric field. A peak field of ~3 MV/m is at the anode in the cylindrical chamber, whereas a parallel-plate geometry would produce only ~1 MV/m matching these discharge parameters. In addition, the anode is a threaded rod, whose points further enhance the field locally above and beyond 3 MV/m. Another potential cause of ignition near the anode is a plasma-induced local increase in the concentration of atomic oxygen in the mixture, where the high currents of the transient plasma remove, at least partially, the electrode's surface oxide layer. This local generation of oxygen would enhance combustion near the anode. A final postulate is that the plasma discharge likely heats the anode. This heating may assist the combustion reactions by providing the heat needed to assist local ignition along the anode. Further study is needed in order to determine why ignition initiates along the electrode and if ignition within the chamber volume is possible with increasing the reduced electric field.
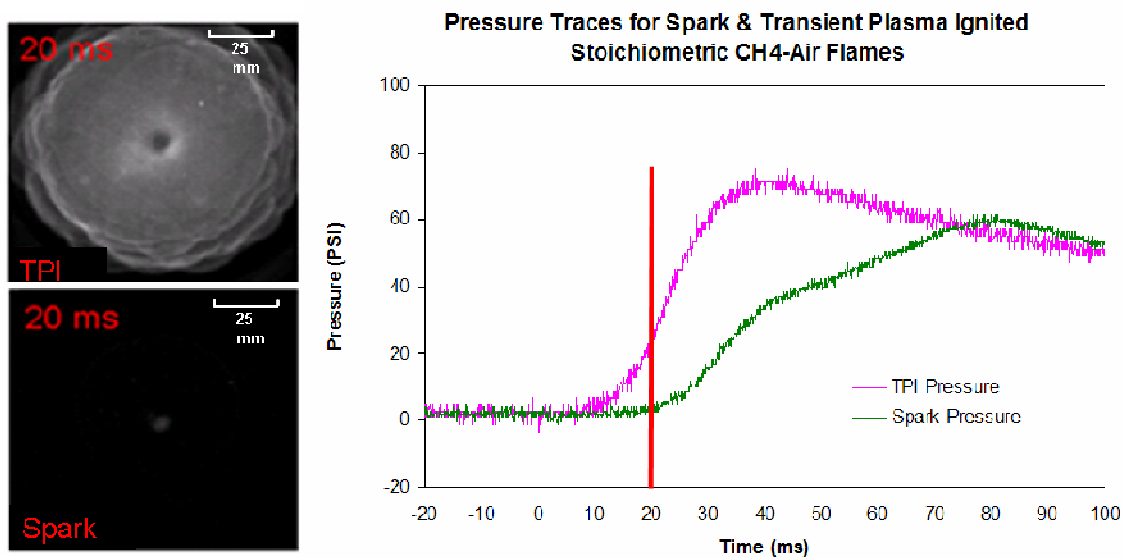

Figure 7. Visible flame propagation for transient plasma and spark ignited CH4–air, $\phi = 1$ mixtures at t = 20 ms, along with associated pressure traces.

Figure 7 shows flame propagation 20 ms after transient plasma/spark ignition and the temporal pressure response for both ignition sources. The ignition delay time (time it takes to reach 10% of the peak pressure) for a TPI flame is 34% smaller than that of the spark ignited flame. With a smaller diameter chamber, a factor of 3 reduction has been observed for TPI.[18] Additionally, the peak pressure for the TPI was higher. The transient plasma combustion reached 6.7 atm, whereas the spark-induced flame reached only 6.3 atm. Lastly, the rise time from 10% – 90% was 59% shorter for the transient plasma case. It is important to note that the transient plasma was delivering ~800 mJ, whereas the spark was delivering ~40 mJ.

This faster and earlier rise in pressure for the TPI case does not necessarily suggest a rise in flame speed. When the high speed camera images of the flame front were analyzed to estimate the flame speed with transient plasma ignition, it was found to be ~40 cm/sec, which is very close to the accepted value for a laminar stoichiometric flame. The faster rise time is then likely due to the multiple ignition points for the TPI case. This indicates that the OH seen in the first 100μs of the discharge has little or no effect on flame propagation, as ignition does not occur until well after the OH number density decays, and the flame propagation does not change from conventional ignition.

IV. Conclusions

The transient plasma produces OH radicals throughout the streamer paths. Under the conditions tested within a chamber filled with a 1 atm mixture of stoichiometric CH_4 and dry air, OH decayed rapidly, falling below the LIF detection limit within 100 μs, while ignition did not occur for another 900 μs. Therefore, OH produced by the plasma in the bulk of the chamber had no immediate effect on ignition. Ignition delay is reduced from ~10 ms for the spark ignition to ~1 ms for the transient plasma. However, the flame takes approximately 20 ms to traverse the cylinder radius for both ignition cases. Estimations of flame speed show that fluid composition influenced by the plasma streamers did not enhance the speed of flame propagation. Ignition always occurred solely along the anode, creating an outwardly propagating cylindrical flame.

These results taken together suggest that the fluid in close proximity to the anode needs further study. The peak field density near the anode may allow enough radicals to be produced during the discharge for ignition to occur; however, the time decay of OH in the PLIF images suggests additional potential chemical processes. This may include the removal of the anode oxide layer, locally enhancing the combustion process, or local elevation of gas temperature by joule heating of the electrode during the discharge. The potential for electrode material effects on ignition could provide an interesting avenue for ignition control.

Acknowledgments

References

[1] C. Cathey, F. Wang, T. Tang, A. Kuthi, M. A. Gundersen, J. Sinibaldi, C. Brophy, J. Hoke, F. Schauer, J. Corrigan, J. Yu, E. Barbour, and R. Hanson, "Transient Plasma Ignition for Delay Reduction in Pulse Detonation Engines," Paper AIAA-2007-443, 45th AIAA Aerospace Sciences Meeting and Exhibit, Reno, NV, Jan. 2007.

[2] S. Pancheshnyi, M. Nudnova, and A. Starikovskii, "Development of a cathode-directed streamer discharge in air at different pressures: Experiment and comparison with direct numerical simulation," Physical Review E , Vol. 71 (2005) 016407.

[3] N. L. Aleksandrov, N. B. Anikin, E. M. Bazelyan, D. V. Zatsepin, S. M. Starikovskaia, and A. Yu. Starikovskii, "Chemical reactions and ignition initiation in hydrocarbon-air mixtures by high-voltage nanosecond gas discharge." Paper AIAA 2001-2949, 4th Weakly Ionized Gases Workshop, Anaheim, CA, 2001.

[4] I. Glassman, Combustion, 3rd ed., Academic Press 1996.

[5] S. M. Starikovskaia, "Plasma assisted ignition and combustion," J. Phys. D: Appl. Phys., Vol. 39 (2006) R265–R299.

[6] C. Cathey, T. Tang, A. Kuthi, M. A. Gundersen, T. Shiraishi, and T. Urushihara, "Nanosecond plasma initiated processes for improved combustion," IEEE Transactions on Plasmas, in press.

[7] F. Wang, A. Kuthi, and M. A. Gundersen, "Compact high repetition rate pulse generator," IEEE Transactions on Plasma Science, Vol. 33 (2005), 1177-1181.

[8] R. S. Barlow, A. N. Karpetis, J. H. Frank, and J.-Y. Chen, "Scalar profiles and NO formation in laminar opposed-flow partially premixed methane/air flames," Combustion and Flame, Vol. 127, (2001), 2102–2118.

[9] T. Ombrello, X. Qin, ,Y. Ju, A.Gutsol, A. Fridman, and C. Carter, "Combustion enhancement via stabilized piecewise nonequilibrium gliding arc plasma discharge," AIAA Journal, Vol. 44 (2006), 142-150.

[10] J. Luque and D. R. Crosley, "Transition probabilities in the $A^2\Sigma^+ – X^2\Pi$ electronic system of OH," J. Chem. Phys., Vol. 109 (1998) 439-448.

[11] K. L. Steffens, and D. R. Crosley, "Vibrational energy transfer in OH $A^2\Sigma^+$ between 195 and 295 K," J. Chem. Phys., Vol. 112 (2000), 9427-9432.

[12] M. Köllner, P. Monkhouse, and J. Wolfrum, "Time-resolved LIF of OH($A^2\Sigma^+$, v′=1 and v′=0) in atmospheric-pressure flames using picosecond excitation," J. Chem. Phys. Lett., Vol. 168, (1990) 355-360.

[13] P. H. Paul "Vibrational energy transfer and quenching of OH $A^2\Sigma^+$(v′=1) measured at high temperatures in a shock tube," J. Phys. Chem., Vol. 99 (1995) 8472-8476.

[14] D. A. Kliner and R. L. Farrow, "Measurements of ground-state OH rotational energy-transfer rates," J. Chem. Phys., Vol. 110 (1999) 412-422.

[15] J. Burris, J. J. Butler, T. J. McGee, and W. S. Heaps, "Collisional deactivation rates for $A^2\Sigma^+$(v′=1) state of OH," Chem. Phys., Vol. 124 (1988) 251-258.

[16] G. Zizak, G. A. Petrucci, C. L.,Stevenson, and J. D. Winefordner, "Ground state saturated population distribution of OH in an acetylene-air flame measured by two optical double resonance pump-probe approaches," Appl. Opt., Vol. 30 (1991) 5270-5275.

[17] R. Abu-Gharbieh, G. Hamarneh, T. Gustavsson, and C. Kaminski, "Flame front tracking by laser induced fluorescence spectroscopy and advanced image analysis," Optics Express, Vol. 8 (2001) 278-287.

[18] J. Liu, F. Wang, L. C. Lee, P. D. Ronney, and M. A. Gundersen, "Effects of fuel type on flame ignition by transient plasma discharges," Paper AIAA-2004-0837, 42nd AIAA Aerospace Sciences Meeting and Exhibit, Reno, NV, Jan 2004.